

ARTICLE

DOI: 10.1038/s42004-018-0040-0

OPEN

Straightforward access to linear and cyclic polypeptides

Yu Zhang¹, Renjie Liu¹, Hua Jin¹, Wenliang Song¹, Rimesh Augustine¹ & Il Kim ¹

Ring-opening polymerization of α -amino acid *N*-carboxyanhydrides (NCAs) is a powerful synthetic methodology for generating well-defined functional polypeptides. However, conventional procedures require a compromise between obtaining controlled microstructures and employing the optimized polymerization conditions. Specifically, a versatile method to access sequenced cyclic polypeptides remains challenging due to the difficulty in site-specific cyclization. Here we describe a general and straightforward method for the synthesis of both linear and cyclic polypeptides using organocatalytic living polymerization of NCAs. The use of an air-stable organocatalyst, imidazolium hydrogen carbonate, allows for the rapid and controlled polymerization of a variety of NCAs, leading to high conversion within a few minutes under mild conditions. Linear and cyclic block copolypeptides are also accessible simply by controlling the type of initiators and the order of addition of NCA monomers.

¹BK21 PLUS Centre for Advanced Chemical Technology, Department of Polymer Science and Engineering, Pusan National University, Pusan 609-735, Republic of Korea. Correspondence and requests for materials should be addressed to I.K. (email: ilkim@pusan.ac.kr)

The desire to harvest the tunable and biomimetic functionality of biomedical macromolecules through synthetic analogues has spawned the development of polypeptide-based hybrid materials^{1–3}. The remarkable applications of polypeptides in drug delivery, tissue engineering, sensing, and catalysis have simulated considerable efforts to develop routes for the synthesis of polypeptides with the desired structural and functional capabilities^{4–8}. Work toward this end has mainly been pioneered by Deming and co-workers^{9–11}. The ring-opening polymerization (ROP) of α -amino acid *N*-carboxyanhydrides (NCAs), initiated by amines or amine-derivatives (e.g., amine hydrochlorides^{12,13}, amine trifluoroboranes¹⁴, and silazane derivatives^{15,16}), has emerged as a versatile method due to their advantages, including being a metal-free procedure and the absence of any toxic impurities. Intensive mechanistic studies have shown that two competitive mechanisms (the normal amine mechanism and the activated monomer mechanism) lead to undesirable side reactions, preventing the formation of well-defined polypeptides with controlled molecular weights (MWs) and low polydispersity index (\mathcal{D})^{17,18}. Moreover, this method is heavily time-dependent as polymerization usually proceeds over the course of more than 3 days. Although innovations employing new catalysts and/or optimized polymerization conditions have circumvented these problems^{19,20}, these strategies are usually subject to a trade-off between obtaining controlled macromolecules and employing the optimized polymerization conditions: effective catalysts or high vacuum techniques may accelerate the polymerization, but also promote side reactions, making the system essentially impractical. Thus, the synthesis of polypeptides in a controlled manner and the avoidance of time-consuming processes remain formidable challenges.

Despite the crowning achievements in macromolecular topologies and manipulation of the thermal behaviour of linear polymers, exhaustive understanding of the cyclic analogues remains a work in progress. Their distinctive topological architecture imparts many characteristic properties to cyclic polymers, compared to their linear counterparts, such as novel micellar morphology, faster crystallization rate, lower intrinsic viscosity, and higher glass transition and melting temperature^{21–24}. Variety of cyclic peptides have been discovered in nature and have various applications such as antibiotics and immunosuppressive agents. Zwitterionic ROP has recently been recognized as a fundamental strategy for the synthesis of cyclic polymers^{25,26}. This appealing approach enables the generation of cyclic polypeptides (*c*PPePs), initiated by protic nucleophiles (pyridine, imidazole)²⁷. Unexpectedly rapid precipitation of β -sheet lamellae of poly(*L*-alanine) prevented efficient cyclization and generated predominantly linear poly(*L*-alanine). Although a previously reported thermal technique can be used to generate cyclic polypeptides, this method is inherently limited by the type of NCA²⁸. An efficient and facile strategy to access *c*PPePs with defined MWs is thus highly desirable.

In the wake of the pioneering study by Waymouth and co-workers, *N*-heterocyclic carbene (NHC)-mediated ROP of a variety of heterocyclic monomers has led to substantial advances in organocatalysis^{29–32}. Extensive research has shown that persistent NHCs are privileged organocatalysts for metal-free polymerization because of their unique chemical characteristics, i.e., strong σ -donor and good Brønsted base properties^{33,34}. We thus envisioned to employ organocatalysts in ROP of NCAs that have never been explored in polypeptide chemistry. Daniel et al. recently reported that free NHCs can be easily released from imidazolium hydrogen carbonates (denoted as [NHC(H)(HCO₃)] precursors via the formal loss of H₂CO₃^{35,36}, whereas this type of easier-to-handle and air-stable precatalysts have been hitherto poorly studied, especially for polymerization purposes.

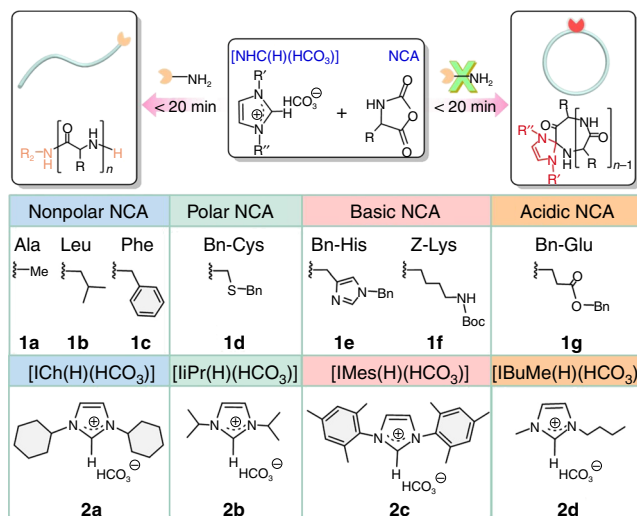


Fig. 1 Ring-opening polymerization of various NCAs. Synthesis of linear and cyclic polypeptides by using [NHC(H)(HCO₃)] with diverse steric and electronic properties

Herein, we present the [NHC(H)(HCO₃)]-mediated ROP of a broad scope of NCAs to access both linear polypeptides (*l*PPePs) and *c*PPePs in the presence and absence of a primary amine initiators, respectively (Fig. 1). Notably, the polymerization occurs very rapidly and high conversion is achieved within a few minutes under the well-optimized conditions. Moreover, linear and cyclic block copolypeptides are easily accessible by tuning the type of initiator and by sequential addition of monomers. This bifunctional organocatalysis strategy was developed based on the conjecture that^{25,34,37} free NHCs can form a hydrogen bonding network with the initiating amines and the subsequently formed ω -amino terminus of the propagating chains (Fig. 2). This H-bonding interaction facilitate nucleophilic attack on the NCAs, thereby resulting in the rapid generation of *l*PPePs.²¹ While in the absence of amines, free NHCs might behave as a sole nucleophile to initiate NCAs and generate the imidazolium carbamate zwitterionic intermediate, allowing for subsequent intramolecular decarboxylation and chain propagation to yield *c*PPePs.

Results

Synthesis and characterization of polypeptides. As depicted in Fig. 2, free NHCs are released at room temperature from its [NHC(H)(HCO₃)] precursor by formal loss of H₂CO₃³⁵. In the presence of a primary amine, the NHCs act as potent organocatalysts for the ROP of four representative types of NCAs (those with nonpolar side chains, benzyl or benzyloxy carbamate protected polar, basic, and acidic side chains), generating respective linear polypeptides with controlled MWs and low \mathcal{D} values (Table 1, entries 1–7). ¹H NMR spectroscopy analysis corroborated the *l*PPep structure with primary amino end groups (Supplementary Figures 1–7). While, in the absence of amine initiators, *c*PPePs with tunable ring sizes (degree of polymerization (DP) = 20–300) were also obtained (Table 1, entries 14–23), where the [NHC(H)(HCO₃)] served as the sole initiator. ¹H NMR spectra and electrospray ionization mass spectra (ESI MS) of the purified product clearly confirmed the proposed polymeric backbone with an NHC moiety affixed to the ring (Supplementary Figures 15–20 and 32). The ¹H–¹H homonuclear correlation spectroscopy (COSY) of two poly(*L*-phenylalanine) samples independently prepared from **2b** mediated ROP of **1c** in the presence and absence of hexylamine (HxA) reveal the same phenylalanine unit, but entirely different initiator signals in

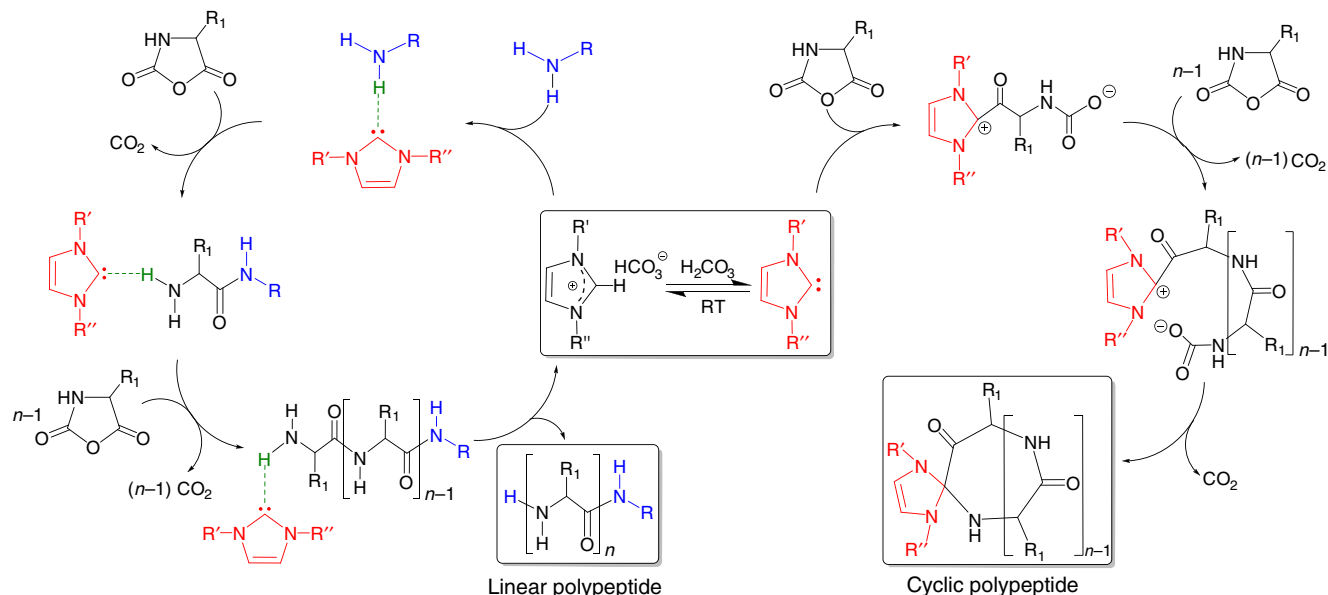


Fig. 2 Proposed mechanism. Bifunctional organocatalysis strategy for $[\text{NHC(H)(HCO}_3\text{)}]$ mediated ROP of NCAs to access both linear and cyclic polypeptides in the presence and absence of a primary amine, respectively

Table 1 Results of controlled ROP of various NCAs with $[\text{NHC(H)(HCO}_3\text{)}]$

Entry	NCA ^a	[I] ^b	p-NHC ^c	$[\text{M}]_0/[\text{I}]_0/[\text{p-NHC}]_0^d$	Time (min)	Conv. ^e (%)	M_n (kg mol ⁻¹)			\bar{D}^g
							Theo. ^f	NMR ^e	SEC ^g	
1	1a	BnA	2b	50:1:0.2	5	53	3.6	1.9	n.d. ^h	n.d.
2	1b	BnA	2b	50:1:0.2	5	42	5.7	2.4	n.d.	n.d.
3	1c	HxA	2b	50:1:0.2	8	63	7.4	4.7	n.d.	n.d.
4	1d	OtA	2b	50:1:0.2	8	67	9.7	6.5	n.d.	n.d.
5	1e	HxA	2b	100:1:0.2	15	79	22.8	18.0	20.2	1.23
6	1g	HxA	2b	100:1:0.2	10	99	22.0	21.8	21.3	1.10
7	1f	HxA	2b	50:1:0.2	20	98	13.2	12.9	14.6	1.17
8	1f	PE	2b	50:1:0.2	30	94	13.8	13.0	n.d.	n.d.
9	1g	HxA	2a	100:1:0.2	10	98	22.0	21.7	22.5	1.17
10	1g	HxA	2c	100:1:0.2	10	97	22.0	21.4	20.7	1.25
11	1g	HxA	2d	100:1:0.2	10	96	22.0	21.1	22.9	1.20
12	1f	HxA	2b	50:1:0.5	20	96	13.2	12.4	13.9	1.18
13	1f	HxA	2b	50:1:1	20	97	13.2	12.8	14.4	1.19
14	1d	—	2b	20:0:1	5	27	4.0	1.1	n.d.	n.d.
15	1c	—	2b	20:0:1	7	55	3.0	1.7	n.d.	n.d.
16	1a	—	2b	50:0:1	9	78	3.7	2.9	n.d.	n.d.
17	1g	—	2b	20:0:1	10	96	4.5	4.3	4.4	1.24
18	1g	—	2b	50:0:1	10	96	11.1	10.7	10.6	1.15
19	1g	—	2b	80:0:1	20	97	17.6	17.0	19.4	1.18
20	1g	—	2b	100:0:1	10	96	22.1	21.2	23.6	1.18
21	1f	—	2b	100:0:1	20	81 ⁱ	26.3	—	21.2 ⁱ	1.30
22	1g	—	2b	200:0:1	60	85	43.9	37.1	42.5	1.15
23	1g	—	2b	300:0:1	60	77	65.8	51.2	40.7	1.13

^aAll polymerizations were carried out in DMF, except for that with PE, which was dissolved in CHCl_3/DMF solution. $[\text{M}]_0 = 0.2 \text{ M}$ for all polymerizations.

^bBnA (benzylamine), HxA (*n*-hexylamine), OtA (*n*-octylamine), and PE (phosphatidylethanolamine) were introduced to entries 1–13 respectively

^cType of $[\text{NHC(H)(HCO}_3\text{)}]$ as shown in Fig. 1, denoted as p-NHC

^d $[\text{M}]_0/[\text{I}]_0/[\text{p-NHC}]_0$ represents the initial molar ratio of the components

^eConversion and experimental MWs were calculated from the ^1H NMR spectrum

^fTheoretical MWs were calculated from the initial molar ratio assuming a single site initiation and complete conversion

^gPolydispersity index determined by SEC calibrated with polystyrene standards

^hNot detected due to the low solubility in DMF

ⁱCalculated by SEC because methyl peak of **2b** overlapped with alkyl side chain of **1f** in ^1H NMR spectrum

upfield (Fig. 3). In order to get further insight into the mechanism of this protocol, we investigated the chain-end groups of these two independently produced polypeptides by matrix-assisted laser desorption/ionization-time of flight mass spectroscopy (MALDI-TOF MS), respectively. The MALDI-TOF MS spectra

(Fig. 4 and Supplementary Figures 33–38) reveal two series of well-distinguishable molecular ion peaks, which correspond to the lPPePs with amino chain ends and the cPPePs bearing an NHC moiety, respectively. More specifically, the spectra for cPPePs detected by using dithranol matrix (Fig. 4c, d and

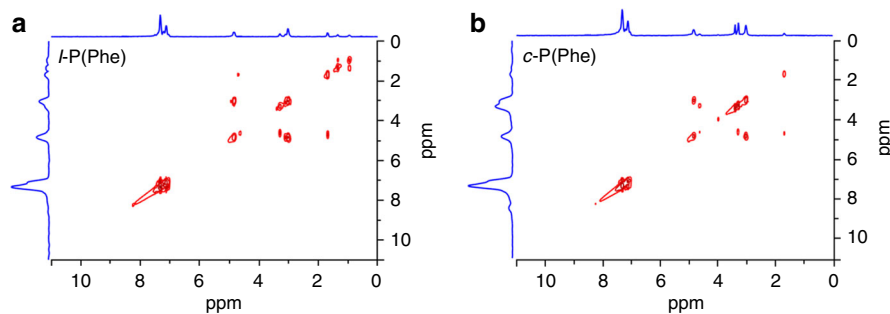


Fig. 3 ^1H – ^1H COSY spectra of polypeptides. **a** Linear poly(L-phenylalanine) (*l*-P(Phe)). **b** Cyclic poly(L-phenylalanine) (*c*-P(Phe))

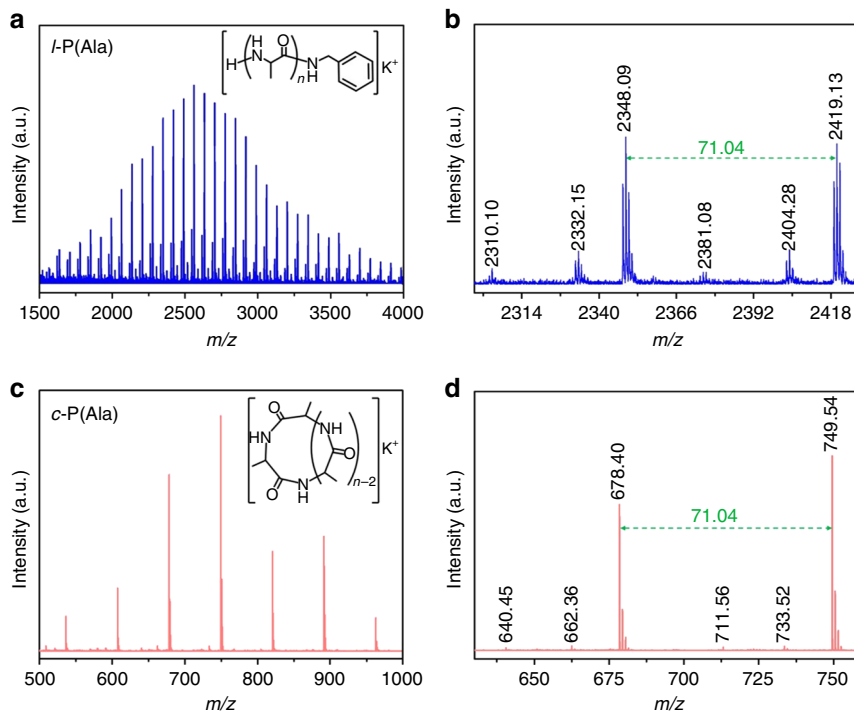


Fig. 4 MALDI-TOF MS spectra of polypeptides. **a** Linear poly(L-alanine) (*l*-P(Ala)). **c** Cyclic poly(L-alanine) (*c*-P(Ala)) using dithranol matrix. **b, d** are the expanded spectra of (**a**), (**c**), respectively

Supplementary Figures 34–37) exhibit signals corresponding to “liberated” polypeptides that the NHC was dissociated from the macrocycles³⁸, whereas structurally intact spirocyclic polypeptides are observed in Supplementary Figure 38 (by using 2,5-dihydroxybenzoic acid matrix). These results are consistent with the mechanistic scenario outlined in Fig. 2.

Remarkably, all polymerizations are featured by high conversion at a significantly high rate, demonstrating the powerful mediating competence of the $[\text{NHC}(\text{H})(\text{HCO}_3)]$. Under optimal conditions, benzylamine-initiated polymerization of **1a** reached 53% conversion in less than 5 min (entry 1 in Table 1). Both polymerizations of **1g** in the presence and absence of HxA proceeded over 96% conversion after 10 min (Table 1, entries 6, 20).

Further evidence for the cyclic architecture of the resulting polypeptides was provided by using size-exclusion chromatography (SEC) with light-scattering, refractive index, and viscosity triple detection. Linear poly(γ -benzyl-L-glutamate) (*l*-PBLG) with $M_n = 17.8 \text{ kg mol}^{-1}$ and $\bar{D} = 1.07$ was prepared using a $[\mathbf{1g}]_0/[\text{HxA}]_0/[\mathbf{2b}]_0$ ratio of 80:1:0.2, whereas the cyclic analogue (*c*-PBLG) with $M_n = 19.4 \text{ kg mol}^{-1}$ and $\bar{D} = 1.18$ was synthesized using a $[\mathbf{1g}]_0/[\mathbf{2b}]_0$ ratio of 80:1 (Supplementary Table 1). As expected, the *c*-PBLGs eluted later and exhibited lower

intrinsic viscosities than their linear analogues with similar MWs, which can be attributed to the smaller hydrodynamic volume of the cyclic topology (Fig. 5a). From the linear fits of the respective Mark–Houwink plot for the cyclic and linear PLBGs, the observed $[\eta]_{\text{cyclic}}/[\eta]_{\text{linear}}$ ratio (approximately 0.79) deviated somewhat from the theoretical prediction for cyclic polymers (0.7)^{29,39,40}, most probably due to the residual linear contaminants present in the mostly cyclic polymers (Fig. 5b). The nearly identical exponent values in the Mark–Houwink plot (0.81 versus 0.77) revealed both polymers possessing a random coil conformation in solution. However, the circular dichroism (CD) analysis for both polymers shows double peaks in the negative region at approximately $\lambda = 200\text{--}220 \text{ nm}$ (Fig. 5c), indicating the α -helix conformation of the PBLG backbone. The inconsistency of these two results may be ascribed to the polypeptide taking an imperfect helix in solution, which makes the α -helix depart from rigid rectilinearity and shows flexibility to some extent⁴¹. Hence, all results excluded possible conformational effects as being responsible for the intrinsic viscosity differences.

To assess the versatility of the $[\text{NHC}(\text{H})(\text{HCO}_3)]$ -mediated ROP of NCAs, we investigated the polymerization of **1f** (entry 8

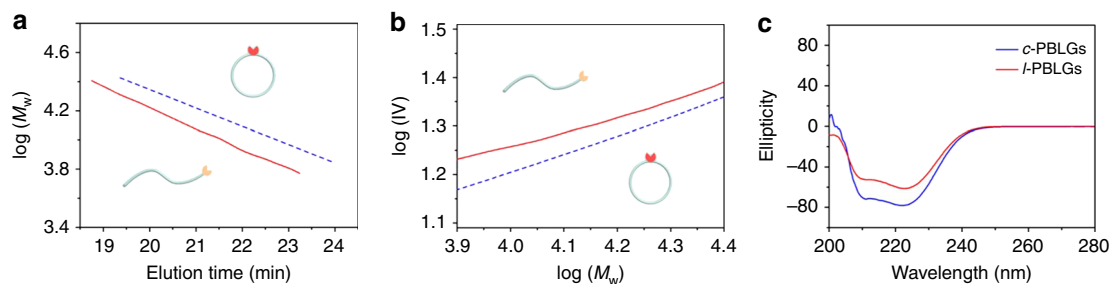


Fig. 5 Topology analysis. **a** Logarithmic plot of MW ($\log M_w$) versus elution time. **b** Mark–Houwink plot for *l*-PBLGs (red line) and *c*-PBLGs (blue line). **c** CD spectra of *l*-PBLGs (red line) and *c*-PBLGs (blue line) with a concentration of 0.2 mg mL^{-1} in THF

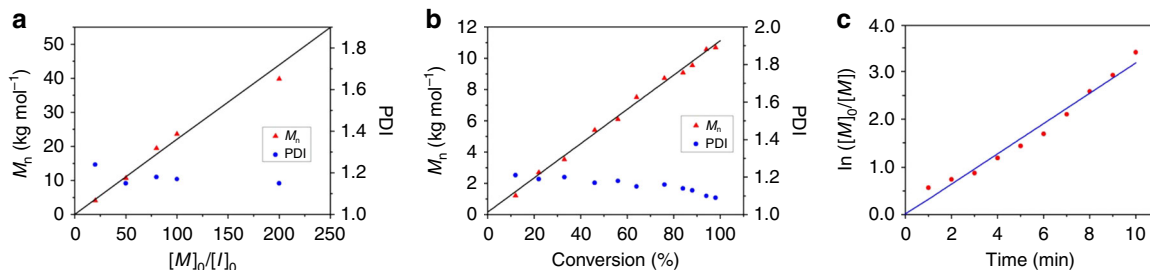


Fig. 6 Kinetic study. **a** Plot of M_n and \bar{D} versus monomer/initiator ($[M]_0/[I]_0$) ratio. **b** Plot of M_n and \bar{D} versus monomer conversion for *c*-PBLG ($[M]_0/[I]_0 = 50:1$, $[M]_0 = 0.3 \text{ M}$). **c** Kinetic plot of $\ln([M]_0/[M])$ versus time for *c*-PBLG ($[M]_0/[I]_0 = 50:1$, $[M]_0 = 0.3 \text{ M}$)

in Table 1) using phosphatidylethanolamine (PE) as an initiator, resulting in an attractive synthesis of the PE-*b*-poly (Z-Lys) (PE-*b*-PZLL) bioconjugate. The ^1H NMR spectra confirmed the formation of the desired chimeric bioconjugate (Supplementary Figures 8, 9). Methoxypolyethylene glycol amine (mPEG-NH₂) could also initiate to yield the desired PBLG PEGylated product (Supplementary Figures 10, 11).

In an attempt to broaden the scope of such a prominent precatalyst, several $[\text{NHC}(\text{H})(\text{HCO}_3)]$ precursors with diverse steric and electronic properties were utilized to mediate the ROP of **1g** (Table 1, entries 6, 9–11). Intriguingly, the controlled polymerizations yielded linear polypeptides with predictable MWs and $\bar{D} < 1.3$, indicating that all of these promising $[\text{NHC}(\text{H})(\text{HCO}_3)]$ precatalysts permit excellent control over MW and \bar{D} . Besides, the effect of the initial $[\text{NHC}(\text{H})(\text{HCO}_3)]$ concentration on control of the MW of the linear polymers was evaluated for the polymerization of **1f** with varying concentrations of **2b** and keeping initial monomer and HxA concentrations constant under the standard conditions (Table 1, entries 7, 12, and 13). The minor variation of MW with $[\mathbf{2b}]_0$ concentration implies that **2b** simply acts as an effective catalyst to promote the polymerization. Additionally, the protected groups can be easily deprotected by treating with HBr in trifluoroacetic acid, as exemplified by linear PBLG, PZLL, and PE-*b*-PZLL (Supplementary Figures 12–14).

Kinetic study. $[\text{NHC}(\text{H})(\text{HCO}_3)]$ had remarkable control over most of polymerizations tested. Taking **2b**-mediated ROP of **1g** as an example (Fig. 6a), the resultant *c*-PBLGs display linearly increased MWs, nearly identical to the expected MWs, as the feeding monomer/initiator $[M]_0/[I]_0$ ratios from 20 to 200. At $[M]_0/[I]_0$ ratio of 300/1, the obtained DP was about 233, nearly 22.4% deviation from the expected DP (as shown in Table 1, entry 23). Furthermore, the MWs of *c*-PBLG increase linearly with the conversion of **1g** (Fig. 6b), verifying the living nature of polymerizations. Preliminary kinetic investigations of *c*-PBLG further corroborate the living character. The plot of $\ln([M]_0/[M])$ versus time fits well to a linear theoretical line, suggesting that

the polymerization proceeds with a first-order kinetic character on the **1g** concentration and gives the observed polymerization rate constant $k_{\text{obs}} = 0.265 \pm 0.01 \text{ min}^{-1}$ (Fig. 6c). All these experimental data confirmed that the ROP of **1g** mediated by **2b** proceeded in a controlled/living way. Similar living feature was also observed for *l*-PBLGs, as evidenced by the control experiments for the polymerization of **1g** in the presence of HxA (Supplementary Figure 39).

Copolymerization of Bn-Glu NCA and Z-Lys NCA. In analogy with the living feature of the propagating chains, a chain extension experiment was conducted by utilizing the *c*-PBLG (DP = 30) macroinitiator prepared by **2b**-mediated polymerization of **1g** ($[\mathbf{1g}]_0 = 0.2 \text{ M}$, $[\mathbf{1g}]_0/[\mathbf{2b}]_0 = 30:1$). After complete conversion of **1g**, a second batch of **1f** ($[\mathbf{1f}]_0/[\mathbf{2b}]_0 = 70:1$) was added to the reaction mixture to allow for further chain propagation (Supplementary Table 2). ^1H and ^{13}C NMR analyses (Supplementary Figures 21, 22) of the resultant copolymer reveal significant resonance signals for the PZLL unit, as compared to *c*-PBLG. ^1H , ^1H -COSY, and HSQC spectral analyses (Supplementary Figures 23, 24) further confirm the formation of the anticipated cyclic block copolypeptides (*c*-(PBLG-*b*-PZLL)). Based on comparison of *c*-PBLG and *c*-(PBLG-*b*-PZLL), for example, the ^1H , ^1H -COSY spectra present four representative upfield signals for the methylene protons of *c*-(PBLG-*b*-PZLL), strongly suggesting the formation of the anticipated *c*-(PBLG-*b*-PZLL). Encouraged by these initial findings, linear block copolypeptides (*l*-(PBLG-*b*-PZLL), $[\mathbf{1g}]_0/[\mathbf{1f}]_0/[\text{HxA}]_0/[\mathbf{2b}]_0 = 20:60:1:0.2$) were also accessed by using a *l*-PBLG (DP = 20) macroinitiator (Supplementary Figure 25). SEC analysis of the resulting polymers obtained prior to and after the addition of the second monomer shows unimodal distributions and the increase in the MWs of the polymer agreed reasonably well with the theoretically predicted value, suggesting controlled chain extension and successful synthesis of cyclic and linear block copolypeptides (Fig. 7).

Mechanistic insight of $[\text{NHC}(\text{H})(\text{HCO}_3)]$ -mediated ROP. It is well known that the propagation is slow for the normal amine

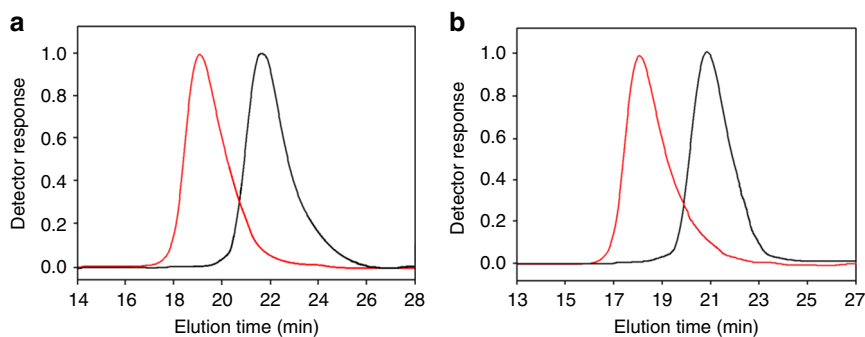


Fig. 7 Chain extension experiment. **a** Representative SEC chromatograms of *l*-PBLG macroinitiator (black curve) and *l*-(PBLG-*b*-PZLL) (red curve). **b** *c*-PBLG Macroinitiator (black curve) and *c*-(PBLG-*b*-PZLL) (red curve)

mechanism due to the weak nucleophilic ω -amino group of the propagating chain²¹. We thus speculate that the aforementioned H-bonding interaction continues activating the subsequently formed ω -amino terminus of the propagating chains, resulting in the rapid generation of *l*PPePs. Toward this end, FT-IR spectra were recorded to verify the existence of H-bonding. As the mole ratio of [2c]/[HxA] increases from 0 to 3 (Supplementary Figure 40), N–H stretching vibration peaks at 3378 cm^{-1} and 3295 cm^{-1} shift to lower wavenumbers, whereas N–H bending vibration peak at 1586 cm^{-1} shifts to higher one. The formation of H-bonding causes the red/blue shifts of N–H stretching/bending vibration^{42,43}. For further demonstrating the H-bonding interaction, ¹H NMR spectra were collected for equimolar mixtures of **2b** and HxA in CDCl₃ at room temperature (Supplementary Figure 26). The equilibrium between **2b** and imidazolium-2-carboxylates is entirely disrupted by the addition of HxA³⁵, accompanied by the disappearance of the signals of the amide protons of HxA at 1.03 ppm and the appearance of a new broad peak at 3.14 ppm, indicative of the H-bonding interaction between **2b** and HxA. To gain deep insight into this new broad peak, variable temperature ¹H NMR spectra of the same mixtures were recorded at temperatures ranging from 25 to 45 °C (Supplementary Figure 27)⁴⁴. The corresponding signal at 3.14 ppm shifts to upfield as temperature increases from 25 to 45 °C, implying the significantly temperature-dependent behaviour of H-bonding interaction. Thus, the results collected support the suggested H-bonding network conjecture. Even though the exact polymerization mechanism for generating *c*PPePs is not clear at this stage, most probably [NHC(H)(HCO₃)] acts as the nucleophile to initiate NCAs.

Discussion

In summary, the [NHC(H)(HCO₃)]-mediated procedure presented in this work not only permits the rapid and efficient synthesis of well-defined polypeptides via an ROP of a variety of NCAs, but also provides control over the polypeptide architecture. The living nature of this process allows for the straightforward access to both linear and cyclic block copolypeptides simply by tuning the type of initiators and by sequential addition of NCAs. More importantly, the [NHC(H)(HCO₃)] salts are versatile and easy-to-handle precatalysts for the precise polypeptides synthesis, without particular precautions of storage. This strategy opens up opportunities for the practical use of these masked NHCs in various NHC-catalysed macromolecular reactions, and enables bulk-scale synthesis, potentially providing an avenue for practical implementation in the design of diverse polypeptide-based hybrid materials. Further efforts are underway to elucidate the mechanistic and kinetic features of this organo-catalysis machinery in detail.

Methods

Synthesis and characterization. See Supplementary Methods, Supplementary Tables 1–3, and Supplementary Figures 1–43 (¹H and ¹³C NMR spectra, MALDI-TOF and ESI MS spectra). The results of independently synthesized NHCs mediated the polymerization of NCAs to generate both linear and cyclic polypeptides are available in Supplementary Figures 28–31 and 43.

General procedures for synthesis polypeptides. Linear polypeptides were synthesized according to the following steps. **1g** (263.25 mg, 1 mmol) was added to the Schlenk flask with 4.5 mL of DMF. Molecular sieves were subsequently added into the reaction mixture to trap the water released from the [NHC(H)](HCO₃). *n*-Hexylamine (2.7 μL , 2×10^{-5} mol) was introduced into the solution, and a predetermined amount of **2b**/DMF stock solution (500 μL , 1×10^{-5} mol, 0.02 M) was then added to the reaction mixture using a syringe. The reaction mixture was stirred for an appropriate time at room temperature and the conversion of NCA was determined by ¹H NMR spectrum of an aliquot of reaction mixture. After the desired period, the polymerization was quenched by adding 10 mL of methanol. The quenched mixture was further precipitated by adding excess amount of methanol. After sonication and centrifugation twice to remove the unreacted monomers, the white solid was dried under vacuum. A similar procedure was employed for the preparation of the cyclic polypeptides in the absence of amine initiators.

General procedures for synthesis copolypeptides. Linear copolypeptides were synthesized according to the following procedures. **1g** polymerization ([**1g**]₀ = 0.2 M, [**1g**]₀/[I]₀ = 20:1, [**2b**]₀ = 2.0 mM) was carried out by the same procedure as mentioned above. Aliquots of the reaction mixture were taken and the MW of the polypeptides was analysed by SEC and the monomer conversion was determined by ¹H NMR. If ([**1g**]₀/[I]₀ = 60:1) dissolved in 2 mL DMF was then added to the solution and the mixture was stirred for an additional 30 min to reach complete conversion. The solution was precipitated with excess methanol. After sonication and centrifugation twice to remove unreacted monomers, the white solid was dried under vacuum to afford the linear block copolypeptides. The final products were analysed by SEC and ¹H NMR. A similar procedure was employed for the preparation of cyclic copolypeptides in the absence of amine initiators.

Data availability. The datasets generated and analysed during the current study are available from the corresponding authors on reasonable request.

Received: 23 April 2018 Accepted: 25 June 2018

Published online: 18 July 2018

References

- Iwane, Y. et al. Expanding the amino acid repertoire of ribosomal polypeptide synthesis via the artificial division of codon boxes. *Nat. Chem.* **8**, 317–325 (2016).
- Estrich, N. A., Hernandez-García, A., De Vries, R. & LaBean, T. H. Engineered diblock polypeptides improve DNA and gold solubility during molecular assembly. *ACS Nano* **11**, 831–842 (2017).
- Baumgartner, R., Fu, H., Song, Z., Lin, Y. & Cheng, J. Cooperative polymerization of α -helices induced by macromolecular architecture. *Nat. Chem.* **9**, 614–622 (2017).
- Hanson, J. A. et al. Nanoscale double emulsions stabilized by single-component block copolypeptides. *Nature* **455**, 85–88 (2008).

5. Ta, D. T., Vanella, R. & Nash, M. A. Magnetic separation of elastin-like polypeptide receptors for enrichment of cellular and molecular targets. *Nano Lett.* **17**, 7932–7939 (2017).
6. Song, Z. et al. Synthetic polypeptides: from polymer design to supramolecular assembly and biomedical application. *Chem. Soc. Rev.* **46**, 6570–6599 (2017).
7. Deming, T. J. Synthesis of side-chain modified polypeptides. *Chem. Rev.* **116**, 786–808 (2015).
8. Fu, J., Yu, C., Li, L. & Yao, S. Q. Intracellular delivery of functional proteins and native drugs by cell-penetrating poly(disulfide)s. *J. Am. Chem. Soc.* **137**, 12153–12160 (2015).
9. Deming, T. J. Facile synthesis of block copolypeptides of defined architecture. *Nature* **390**, 386–389 (1997).
10. Cha, J. N., Stucky, G. D., Morse, D. E. & Deming, T. J. Biomimetic synthesis of ordered silica structures mediated by block copolypeptides. *Nature* **403**, 289–292 (2000).
11. Yakovlev, I. & Deming, T. J. Controlled synthesis of phosphorylcholine derivatives of poly (serine) and poly(homoserine). *J. Am. Chem. Soc.* **137**, 4078–4081 (2015).
12. Vacogne, C. D. & Schlaad, H. Primary ammonium/tertiary amine-mediated controlled ring opening polymerisation of amino acid *N*-carboxyanhydrides. *Chem. Commun.* **51**, 15645–15648 (2015).
13. Dimitrov, I. & Schlaad, H. Synthesis of nearly monodisperse polystyrene–polypeptide block copolymers via polymerisation of *N*-carboxyanhydrides. *Chem. Commun.* **23**, 2944–2945 (2003).
14. Conejos-Sánchez, I., Duro-Castano, A., Birke, A., Barz, M. & Vicent, M. J. A controlled and versatile NCA polymerization method for the synthesis of polypeptides. *Polym. Chem.* **4**, 3182–3186 (2013).
15. Lu, H. & Cheng, J. *N*-trimethylsilyl amines for controlled ring-opening polymerization of amino acid *N*-carboxyanhydrides and facile end group functionalization of polypeptides. *J. Am. Chem. Soc.* **130**, 12562–12563 (2008).
16. Yuan, J., Sun, Y., Wang, J. & Lu, H. Phenyl trimethylsilyl sulfide-mediated controlled ring-opening polymerization of α -amino acid *N*-carboxyanhydrides. *Biomacromolecules* **17**, 891–896 (2016).
17. Hadjichristidis, N., Iatrou, H., Pitsikalis, M. & Sakellariou, G. Synthesis of well-defined polypeptide-based materials via the ring-opening polymerization of α -amino acid *N*-carboxyanhydrides. *Chem. Rev.* **109**, 5528–5578 (2009).
18. Huang, J. & Heise, A. Stimuli responsive synthetic polypeptides derived from *N*-carboxyanhydride (NCA) polymerisation. *Chem. Soc. Rev.* **42**, 7373–7390 (2013).
19. Peng, H., Ling, J. & Shen, Z. Ring opening polymerization of α -amino acid *N*-carboxyanhydrides catalyzed by rare earth catalysts: polymerization characteristics and mechanism. *J. Polym. Sci., Part A: Polym. Chem.* **50**, 1076–1085 (2012).
20. Aliferis, T., Iatrou, H. & Hadjichristidis, N. Living polypeptides. *Biomacromolecules* **5**, 1653–1656 (2004).
21. Zhao, W., Gnanou, Y. & Hadjichristidis, N. From competition to cooperation: a highly efficient strategy towards well-defined (co)polypeptides. *Chem. Commun.* **51**, 3663–3666 (2015).
22. Shin, E. J. et al. Crystallization of cyclic polymers: synthesis and crystallization behavior of high molecular weight cyclic poly(ϵ -caprolactone)s. *Macromolecules* **44**, 2773–2779 (2011).
23. Bielawski, C. W., Benitez, D. & Grubbs, R. H. An “endless” route to cyclic polymers. *Science* **297**, 2041–2044 (2002).
24. Lee, C.-U., Li, A., Ghale, K. & Zhang, D. Crystallization and melting behaviors of cyclic and linear polypeptoids with alkyl side chains. *Macromolecules* **46**, 8213–8223 (2013).
25. Brown, H. A. & Waymouth, R. M. Zwitterionic ring-opening polymerization for the synthesis of high molecular weight cyclic polymers. *Acc. Chem. Res.* **46**, 2585–2596 (2013).
26. Wang, Q., Zhao, W., He, J., Zhang, Y. & Chen, E. Y.-X. Living ring-opening polymerization of lactones by *N*-Heterocyclic Olefin/Al (C_6F_5)₂ Lewis pairs: structures of intermediates, kinetics, and mechanism. *Macromolecules* **50**, 123–136 (2016).
27. Kricheldorf, H. R., Von Lossow, C. & Schwarz, G. Tertiary amine catalyzed polymerizations of α -amino acid *N*-carboxyanhydrides: the role of cyclization. *J. Polym. Sci., Part A: Polym. Chem.* **44**, 4680–4695 (2006).
28. Kricheldorf, H. R., Lossow, C. V., Lomadze, N. & Schwarz, G. Cyclic polypeptides by thermal polymerization of α -amino acid *N*-carboxyanhydrides. *J. Polym. Sci., Part A: Polym. Chem.* **46**, 4012–4020 (2008).
29. Culkun, D. A. et al. Zwitterionic polymerization of lactide to cyclic poly (lactide) by using *N*-heterocyclic carbene organocatalysts. *Angew. Chem. Int. Ed.* **46**, 2627–2630 (2007).
30. Jeong, W., Shin, E. J., Culkun, D. A., Hedrick, J. L. & Waymouth, R. M. Zwitterionic polymerization: a kinetic strategy for the controlled synthesis of cyclic polylactide. *J. Am. Chem. Soc.* **131**, 4884–4891 (2009).
31. Guo, L., Lahasky, S. H., Ghale, K. & Zhang, D. *N*-Heterocyclic carbene-mediated zwitterionic polymerization of *N*-substituted *N*-carboxyanhydrides toward poly(α -peptoid)s: kinetic, mechanism, and architectural control. *J. Am. Chem. Soc.* **134**, 9163–9171 (2012).
32. Brown, H. A., Chang, Y. A. & Waymouth, R. M. Zwitterionic polymerization to generate high molecular weight cyclic poly(carbosiloxane)s. *J. Am. Chem. Soc.* **135**, 18738–18741 (2013).
33. Hopkinson, M. N., Richter, C., Schedler, M. & Glorius, F. An overview of *N*-heterocyclic carbenes. *Nature* **510**, 485–496 (2014).
34. Fèvre, M., Pinaud, J., Gnanou, Y., Vignolle, J. & Taton, D. *N*-Heterocyclic carbenes (NHCs) as organocatalysts and structural components in metal-free polymer synthesis. *Chem. Soc. Rev.* **42**, 2142–2172 (2013).
35. Fèvre, M. et al. Imidazolium hydrogen carbonates as a genuine source of *N*-heterocyclic carbenes (NHCs): Applications to the facile preparation of NHC metal complexes and to NHC-organocatalyzed molecular and macromolecular syntheses. *J. Am. Chem. Soc.* **134**, 6776–6784 (2012).
36. Fèvre, M., Vignolle, J. & Taton, D. Azolium hydrogen carbonates and azolium carboxylates as organic pre-catalysts for *N*-heterocyclic carbene-catalysed group transfer and ring-opening polymerisations. *Polym. Chem.* **4**, 1995–2003 (2013).
37. Wang, L., Chen, J. & Huang, Y. Highly enantioselective Aza–Michael reaction between alkyl amines and β -trifluoromethyl β -aryl nitroolefins. *Angew. Chem. Int. Ed.* **54**, 15414–15418 (2015).
38. Lahasky, S. H., Serem, W. K., Guo, L., Garno, J. C. & Zhang, D. Synthesis and characterization of cyclic brush-like polymers by *N*-heterocyclic carbene-mediated zwitterionic polymerization of *N*-propargyl *N*-carboxyanhydride and the grafting-to approach. *Macromolecules* **44**, 9063–9074 (2011).
39. Piedra-Arroñi, E., Ladavière, C., Amgoune, A. & Bourissou, D. Ring-opening polymerization with Zn (C_6F_5)₂-based Lewis pairs: Original and efficient approach to cyclic polyesters. *J. Am. Chem. Soc.* **135**, 13306–13309 (2013).
40. Hong, M. & Chen, E. Y.-X. Completely recyclable biopolymers with linear and cyclic topologies via ring-opening polymerization of γ -butyrolactone. *Nat. Chem.* **8**, 42–49 (2016).
41. Yang, C. et al. Toroid formation through a supramolecular “cyclization reaction” of rodlike micelles. *Angew. Chem. Int. Ed.* **56**, 5546–5550 (2017).
42. Zhou, Y. et al. Evidences for cooperative resonance-assisted hydrogen bonds in protein secondary structure analogs. *Sci. Rep.* **6**, 36932 (2016).
43. Zhang, K. et al. Nucleobase-functionalized acrylic ABA triblock copolymers and supramolecular blends. *Polym. Chem.* **6**, 2434–2444 (2015).
44. Frost, J. R., Scully, C. C. G. & Yudin, A. K. Oxadiazole grafts in peptide macrocycles. *Nat. Chem.* **8**, 1105–1111 (2016).

Acknowledgements

This work was supported by the Basic Science Research Program through the National Research Foundation of Korea (2015R1D1A1A09057372). The authors also thank the BK21 PLUS Program for partial financial support.

Author contributions

Y.Z., R.L. and I.K. conceived the idea and designed the experiments. Y.Z. and H.J. performed the experiments. Y.Z., W.S., R.A., and I.K. participated in data analyses and discussions. Y.Z. and I.K. co-wrote the manuscript.

Additional information

Supplementary information accompanies this paper at <https://doi.org/10.1038/s42004-018-0040-0>.

Competing interests: The authors declare no competing interests.

Reprints and permission information is available online at <http://npg.nature.com/reprintsandpermissions/>

Publisher's note: Springer Nature remains neutral with regard to jurisdictional claims in published maps and institutional affiliations.



Open Access This article is licensed under a Creative Commons Attribution 4.0 International License, which permits use, sharing, adaptation, distribution and reproduction in any medium or format, as long as you give appropriate credit to the original author(s) and the source, provide a link to the Creative Commons license, and indicate if changes were made. The images or other third party material in this article are included in the article's Creative Commons license, unless indicated otherwise in a credit line to the material. If material is not included in the article's Creative Commons license and your intended use is not permitted by statutory regulation or exceeds the permitted use, you will need to obtain permission directly from the copyright holder. To view a copy of this license, visit <http://creativecommons.org/licenses/by/4.0/>.

© The Author(s) 2018